IN-DEPTH INVESTIGATION OF THE EFFECT OF GAS NITRIDING PARAMETERS ON AISI 304, AISI 316 AND AISI 316L AUSTENITIC STAINLESS STEELS

S. A. Hassona, F. M. Shuaeib and A. F. Al-Khatib

Mechanical Engineering Dept., Faculty of Engineering,
University of Garyounis, Benghazi, Libya

الملخص

يستخدم الصلب الأوستنيتي المقاوم للصدأ نوع AISI 316 و AISI 316L على نطاق واسع (لاستبدال النوع AISI 304 الأكثر شيوعا) في التطبيقات التي تحتاج إلى تعزيز مقاومة التآكل النقري، و من المعروف أيضا أن هذه الأنواع من الصلب تتمتع بمقاومة تآكل و متانة جيدتين غير أن خواصها السطحية رديئة. من ناحية أخرى، تعتبر النتردة بالغاز عملية شائعة الاستخدام للتقسية السطحية و التي يمكن تطبيقها على الصلب الأوستنيتي المقاوم للصدأ بهدف زيادة صلادته السطحية و مقاومته للبلى.

في هذا العمل، تم اختبار تأثير ظروف النتردة بالغاز على الحساسية تجاه التآكل بين الحبيبي في كل من AISI 304 و AISI 316 و AISI 316L بتطبيق اختبار قياسي هو إختبار الإظهار بحمض الأوكساليك، كما تم أيضا استخدام المجهر الضوئي و حيود الأشعة السينية لفحص تأثير عوامل النتردة بالغاز على البنية المجهرية و التركيب الطوري للطبقات المنتردة المتكونة في العينات المقبولة من ناحية إختبار التآكل. بالإضافة إلى إجراء قياسات الصلادة السطحية على هذه العينات. أظهرت نتائج هذه الدراسة أن النتردة بالغاز للصلب المقاوم للصدأ AISI 304 و AISI 316 و AISI 316L تؤدي إلى تكون طبقات منتردة متشابهة في الأنواع الثلاثة و التي تتفاوت في السماكة والتركيب بحسب ظروف النتردة المختلفة. علاوة على ذلك فإنه تحت الظروف التجريبية المطبقة في هذه الدراسة، وجد أن كل من الصلب المقاوم للصدأ المنترد AISI 304 و AISI 316 معرضان للتآكل بين الحبيبي أكثر من الصلب المقاوم للصدأ المنترد AISI 316L خاصة عند درجات حرارة أعلى من 500 درجة مئوية. هذا السلوك لكل من الصلب المقاوم للصدأ AISI 304 و AISI 316 هو غالبا بسبب الترسب بين الحبيبي لكربيدات الكروم أثناء عملية النتردة. كما وجد أن الصلادة السطحية للصلب AISI 316L المنترد يمكن أن تزداد بأكثر من خمس مرات مقارنة بالمعدن غير المعالج و هذا بدوره يرتبط بتحسن ملحوظ في مقاومة البلى.

ABSTRACT

AISI 316 and AISI 316L austenitic stainless steels have been extensively used (to replace the more common AISI 304) in applications requiring enhanced pitting and general corrosion resistance. It is well known that these types have good corrosion resistance and toughness, but poor tribological properties. Gas nitriding is a well established process for surface hardening that can be applied to austenitic stainless steels with the aim of enhancing its surface hardness and wear resistance.

In this work, the effect of gas nitriding conditions on the sensitisation to intergranular corrosion (IGC) in AISI 304, AISI 316 and AISI 3l6L stainless steels

was tested by applying the standard oxalic acid etch test. Optical microscope and X-ray diffraction (XRD) were used to determine the effect of processing parameters on microstructure and phase-composition of the developed nitrided layers in the acceptable specimens, according to IGC test, in the addition to the surface hardness measurements. The results of this study showed that gas nitriding of AISI 304, AISI 316 and AISI 316L stainless steels produces similar nitrided layers in the three types, which varies in thickness and composition according to the different nitriding conditions. Furthermore, under the experimental conditions carried out in this study, it is found that nitrided AISI 304 and AISI 316 are prone to localized intergranular corrosion (IGC) more than the nitrided AISI 316L, particularly at high temperatures (> 500 °C). This behavior in AISI 304 and AISI 316 stainless steels is mainly due to the grain boundary precipitation of chromium carbides during nitriding processing. Finally, it is found that surface hardness of nitrided AISI 316L could be increased by more than five times compared to the untreated material, which has a significant effect in improving the wear performance.

KEYWORDS: Effect of gas nitriding, Austenitic stainless steels; corrosion resistance; Optical microscope; X-ray diffraction

INTRODUCTION

Among the different types of stainless steels, the austenitic types are the most widely used because of their high corrosion resistance in many environmental conditions and good mechanical properties. On the other side austenitic stainless steels have relatively low surface hardness and wear resistance (low tribological performance), which is directly related to their poor mechanical surface properties. In order to improve these properties, austenitic stainless steels should be surface hardened, which cannot be made by using carburizing and quenching heat treatments [1]. As an alternative, nitriding is an effective surface thermochemical treatment, which leads to a significant improvement in the surface hardness, wear resistance and fatigue strength [2]. Nitriding is widely used in automotive, mechanical and aeronautical engineering. Typical nitrided components are gears, crankshafts, camshafts, cam followers, valves parts, die-casting tools, forging dies, aluminum-extrusion dies, extruder screws, injectors and plastic-mould tools (see Figure (1)).
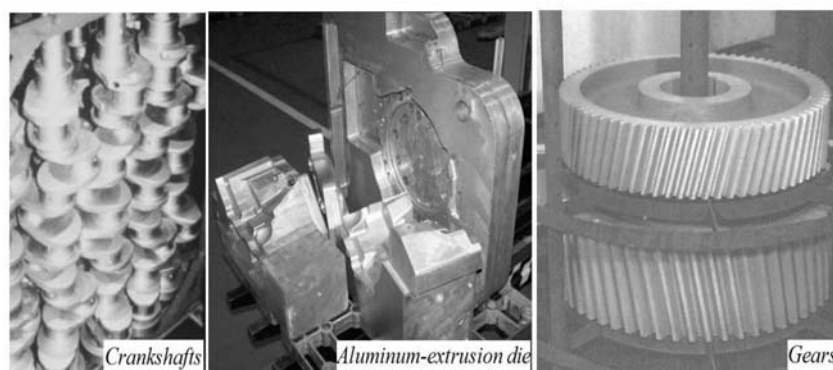

Figure 1: Some nitriding applications

Literature survey on the nitriding of austenitic stainless steels shows that the nitriding process produces a high nitrogen-content surface layer with significant high hardness and improved wear properties [3–7]. The properties and composition of this nitrided layer are strongly influenced by a large number of processing parameters and recently, more research work is directed to study the S-phase, which forms at low nitriding temperatures. This phase is reported to retain the corrosion performance of the nitrided stainless steels [8–10].

However, some heat treatment processes are reported to have diverse effects on the corrosion resistance of stainless steel. Improper heat treatment can produce deleterious changes in the microstructure of austenitic stainless steels and the most troublesome problem is carbide precipitation (sensitization). Intergranular corrosion cracking (IGC) is a direct result of sensitization which occurs when a thermal cycle leads to grain-boundary precipitation of a carbide, nitride, or intermetallic phase without providing sufficient time for chromium diffusion to fill the locally depleted region. The grain-boundary precipitate is not the point of attack; instead, the low-chromium region adjacent to the precipitate is susceptible. One of the developed methods to reduce the risk for intergranular corrosion is by decreasing the level of free carbon in steels. This may be done by either decreasing the carbon content or stabilizing the steel [11, 12].

Therefore in this work, the use of gas nitriding by ammonia to enhance the surface tribological characteristics of AISI 304, AISI 316 and AISI 316L austenitic stainless steels is studied. This study covers the effect of gas nitriding processing parameters on the degree of sensitisation of the substrate austenite matrix and also on the microstructure, composition and surface hardness of the nitrided specimens.

MATERIALS AND METHODS

Three types of commercial austenitic stainless steel have been used as substrate materials with the chemical compositions listed in Table (1). The samples, in the as-received condition, were solution annealed at 1050 °C for 60 minutes followed by oil quench. SiC abrasive papers down to 500-grit were used to manually ground the samples surface to achieve a fine surface finish.

Table 1: Chemical compositions (wt %) of the materials used (Fe balance)

	A		.				.	
X-	A	0.08	0.60	0.01	0.04	1.9	9.5	19.0	-
XI-	A	0.08	0.47	0.02	0.05	1.9	10.0	16.1	2.0
AISI 316L		0.03	0.46	0.02	0.02	1.8	11.2	16.0	2.0

The samples were gas nitrided in the pit type industrial furnace (SIB 572) shown in Figure (2) by using 100% ammonia gas, anhydrous (UN 1005) with a minimum purity of 99.5 %. The nitriding process was conducted with varying three processing parameters which are temperature (°C), time (hr) and ammonia gas flow rate (L/hr). The number of experiments and the processing parameters setting for each experiment were determined using response surface methodology (RSM), one of the design of experiments (DOE) statistical methods, to obtain a proper experimental design with minimum number of experimental points (see Table (2)).
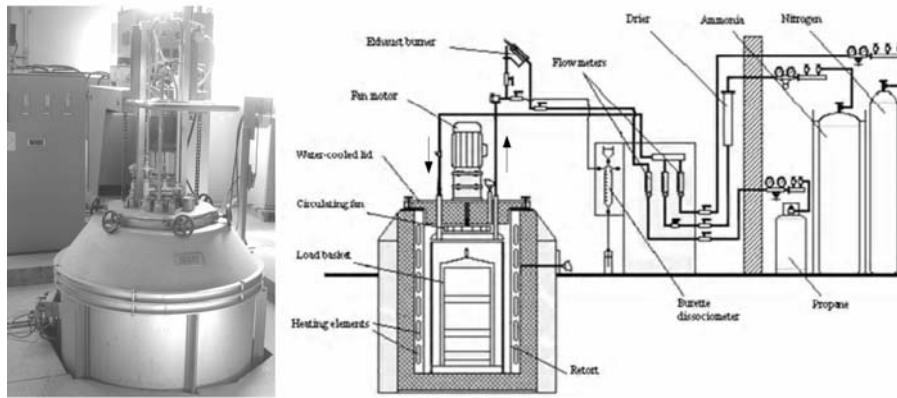
Figure 2: Pit type nitriding furnace

The oxalic acid etch test was used to determine the sensitivity of the nitrided samples to intergranular corrosion (IGC) according to the ASTM A262-86 standard. This test is a rapid method to identify, by simple etching, the specimens that are essentially free of susceptibility to intergranular corrosion attack associated with chromium carbide precipitates [13]. The test is carried out by electrolytically etching the polished specimens for 90 seconds with 1 A/cm^2 current density in 10 % oxalic acid. The surface morphology of the etched specimens are then compared with the standard etch structures classified as shown in Figure (3). According to the standard classification of etch structures only the step and dual structures are acceptable from the view of IGC test [13]. The preparation of nitrided specimens to metallographic examination was carried out with referring to the ASTM E3-80 standard [14]. ZEISS - Axiovert10 light-optical microscope was used to investigate the microstructure of the nitrided layer and substrate while the layer thickness measurements were taken by the micrometer provided with LEICA - VMHT microhardness tester used for the surface hardness measurements. The XRD patterns of nitrided specimens were obtained using PHILIPS - PW1800 x-ray diffractometer with Cu K(radiation and generator setting of 40 kV and 10 mA.
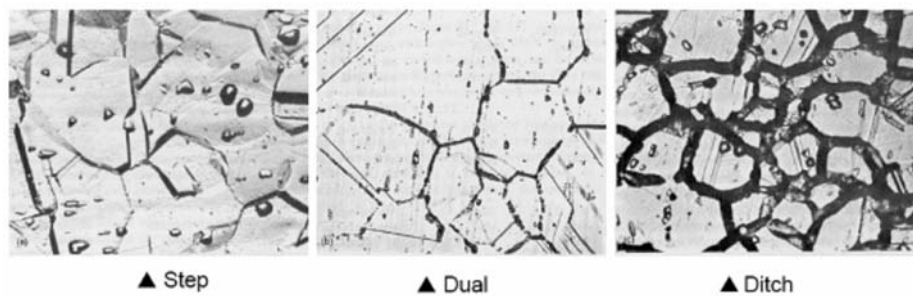

▲ Step   ▲ Dual   ▲ Ditch

Figure 3: Classification of etch structures in oxalic acid etch test [13]

RESULTS AND DISCUSSION
Microstructure Observation

To investigate the morphology of the nitrided layers formed at different process parameters, cross sections from the nitrided samples were examined by optical microscope. The resulted nitrided layers vary in thickness and morphology depending on the nitriding process parameters and the steel chemical composition. In the specimens treated at low temperatures (400 – 440 °C), uniform thin layers were observed in the three alloys which after etching appear bright under microscope, as shown by Figures (4-a), (4-b) and (4-c). At higher magnifications these layers seem to consist of a single phase and are free of precipitation. When the nitriding temperature or time is increased, the bright nitrided layers become speckled with dark spots (Figures (4-d), (4-e) and (4-f)). At higher temperatures of (500 – 600 °C), the layers appear completely dark due to the heavy attack of the etching reagent as shown in Figures (4-g), (4-h) and (4-i).
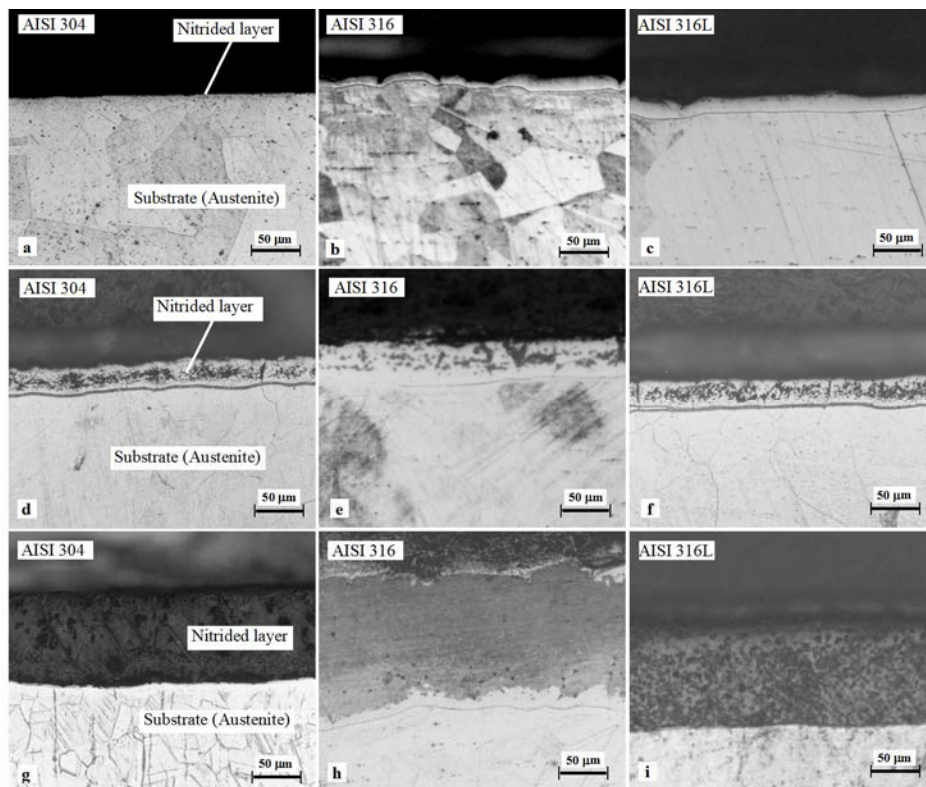

Figure 4: Optical micrographs for nitrided layer morphologies; (a) – (c) design point #11, (d) – (f) design point #9, (g) – (i) design point #14

Layer thickness measurements of the nitrided austenitic stainless steels show comparable values between the three types for same operating conditions. Table (2) lists the layer thickness values, together with the corresponding layer corrosion etch classification and appearance morphologies. From Table (2), it can be seen that as the

nitriding temperature is increased in the range of 400 – 600 °C the resultant layer appearance changes from bright (see Table (2), design points #1, #5 and #11) to mixed (bright / dark) (see Table (2), design points #2, #6 and #9) and then to completely dark (see Table (2), design points #3, #4, #7, #8, #10 and #12 - #15). The same behaviour is observed when the nitriding time is increased from 10 to 50 hr, indicating that the bright layer formed at low temperatures decomposes by increasing nitriding temperature or by prolonged nitriding time. On the other hand, it seems that the flow rate of ammonia has negligible effect on the appearance of the nitrided layer.

Intergranular Corrosion Test

The microstructures of the three types of stainless steels after solution annealing consist of austenitic grains and annealing twins typical of an fcc microstructure with no precipitates detected at the grain boundaries. After performing the oxalic acid etch test (IGC test), the resulting microstructures were classified into three types; step, dual and ditch structures as summarized in Table (2).

Figure (5) shows the etch structures of types AISI 304 and AISI 316 specimens nitrided at three different temperatures. It can be seen from the figure that the specimens nitrided at 400 °C has a step structures and no etch attack is detected at the grain boundaries. On the other side, oxalic acid etch test for the specimens nitrided at 500 °C and 600 °C results in ditch structures and severe attack in the grain boundaries region. For type AISI 316L nitrided specimens, no ditch structures are found in all nitrided specimens and for comparison, the etch structures of AISI 316L specimens nitrided at the same conditions as those shown in Figure (5) are illustrated in Figure (6).

The different results obtained from this test can be explained (based on literature) in light of chromium carbide formation in Cr-Ni austenitic steels [11, 15].

Table 2: Results of microscope investigation and IGC test

design point	Time (hr)	Temperature (°C)	Flow rate (L/hr)	Layer thickness (μm) and (Appearance morphology)			Intergranular corrosion etch classification		
				304	316	316L	304	316	316L
1	18	440	200	4 (B)*	11 (B)	15 (B)	Step	Step	Step
2	42	440	200	20 (M)	25 (M)	23 (M)	Step	Step	Step
3	18	560	200	104 (D)	146 (D)	122 (D)	Ditch	Ditch	Step
4	42	560	200	168 (D)	193 (D)	181 (D)	Ditch	Ditch	Dual
5	18	440	500	7 (B)	17 (B)	18 (B)	Step	Step	Step
6	42	440	500	35 (M)	44 (M)	40 (M)	Step	Step	Step
7	18	560	500	118 (D)	131 (D)	133 (D)	Ditch	Ditch	Step
8	42	560	500	184 (D)	246 (D)	195 (D)	Ditch	Ditch	Dual
9	10	500	350	31 (M)	53 (M)	37 (M)	Ditch	Ditch	Step
10	50	500	350	142 (D)	151 (D)	159 (D)	Ditch	Ditch	Step
11	30	400	350	2 (B)*	8 (B)	10 (B)	Step	Step	Step
12	30	600	350	122 (D)	186 (D)	145 (D)	Ditch	Ditch	Dual
13	30	500	100	96 (D)	106 (D)	90 (D)	Ditch	Ditch	Step
14	30	500	600	108 (D)	144 (D)	123 (D)	Ditch	Ditch	Step
15	30	500	350	96 (D)	100 (D)	78 (D)	Ditch	Ditch	Step
16	30	500	350	91 (D)	118 (D)	88 (D)	Ditch	Ditch	Step
17	30	500	350	88 (D)	107 (D)	82 (D)	Ditch	Ditch	Step
Untreate	-	-	-	-	-	-	Step	Step	Step

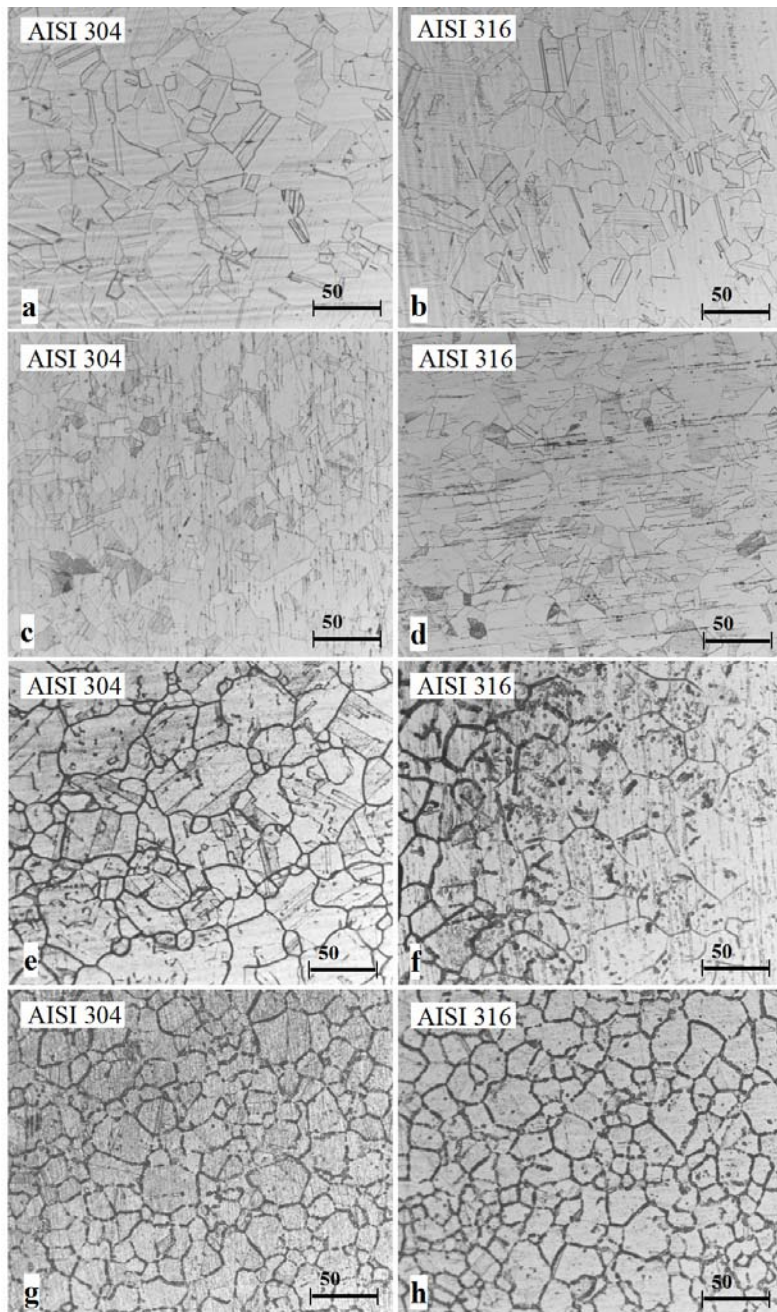(B) Bright layer, (M) Mixed layer, (D) Dark layer, * Discontinuous layer

Figure 5: Optical micrographs after oxalic acid test; (a) & (b) untreated specimen, (c) & (d) design point #11, (e) & (f) design point #15, (g) & (h) design point #12

The ditch structures result from the acid attack at the regions adjacent to the grain boundaries, which are depleted from chromium by the formation of $Cr_{23}C_6$ carbides at austenitic grain boundaries during heating in the sensitization range. Reducing the carbon content in the stainless steel decreases the possibility of $Cr_{23}C_6$ carbides formation and increases the incubation time before sensitisation, which is the case for AISI 316L stainless steel with carbon content of about 0.03%. Therefore, it could be concluded from the previous results that AISI 316L is better than AISI 304 and AISI 316 because of its low carbon content that make it less prone to sensitization (IGC) during the gas nitriding process. However, the specimens of types AISI 304 and AISI 316 when nitrided at temperatures lower than about 500 °C are found to be likely not susceptible to IGC.
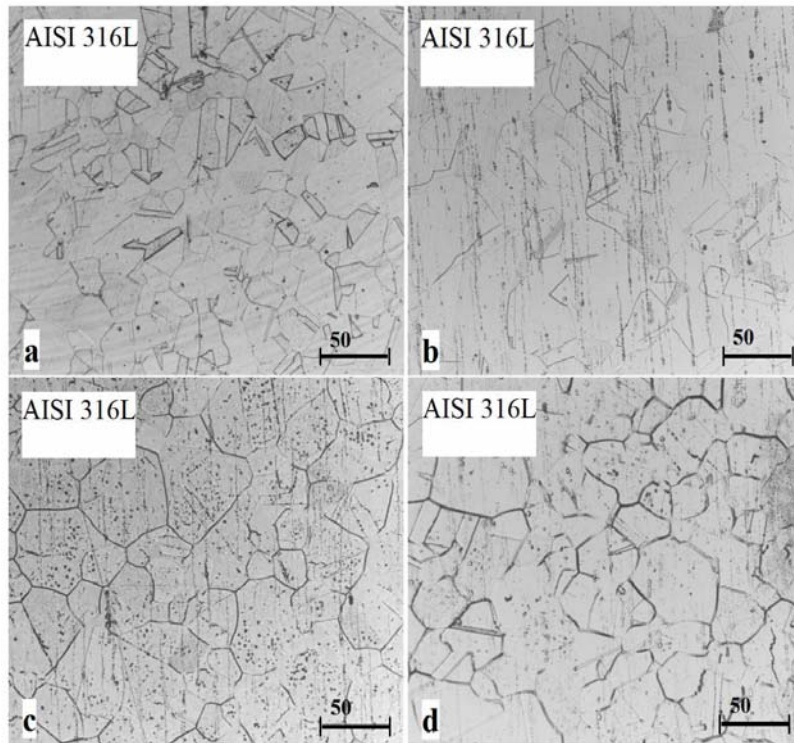

Figure 6: Optical micrographs for AISI 316L after oxalic acid test; (a) untreated specimen, (b) specimen #11, (c) specimen #15, (d) specimen #12

Previous tests that are performed on all the three material types (AISI 304, AISI 316 and AISI 316L) indicate that AISI 316L is superior; hence farther investigations (XRD) are confined to this type of austenitic stainless steel.

X-ray Diffraction Analysis

Using the XRD analysis, the phases present in the nitrided layers of AISI 316L are found to be related to the processing parameters, particularly the nitriding temperature as follows:

First, for the specimens nitrided at temperatures of 400 °C and 440 °C, the XRD patterns are dominated by a set of broad peaks, which appear at lower angles (2γ) as compared to the substrate (untreated) austenite peaks, as shown in Figures (7a) and (7b). These peaks, named S_1, S_2 and S_3 could not be identified by the XRD Index and are identified as expanded austenite (γ_N) or S-phase, as named by several investigators [5,6]. It is noted that the S_2 peak is shifted more than the S_1 peak in relation to the substrate peaks indicating a larger expansion for (200) planes than for (111) planes. Although there is no complete agreement on the nature of S-phase structure [8, 16], many investigators verified the S-phase as a face centered tetragonal (fct) structure with variable lattice parameters according to its nitrogen content [3, 9, 17].
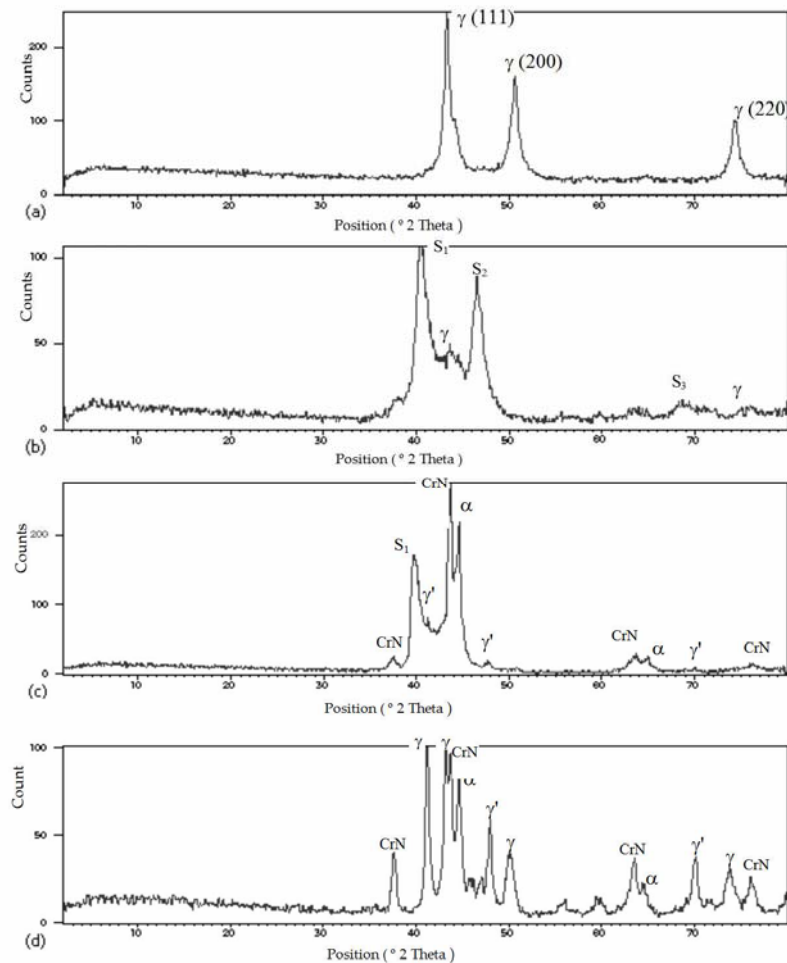

Figure 7: XRD patterns of AISI 316L specimens: (a) untreated, (b) #11, (c) #9, (d) #8

Second, in the XRD patterns of specimens containing mixed (bright/dark) layers, CrN nitride is detected corresponding to the formation of the dark phase in the original bright nitrided layer as shown in Figure (7c). In addition to the CrN peaks, the γ' – Fe₄N nitride, γ (ferrite/martensite) and S-phase peaks are also found. The (bccbc peaks are reported in many studies and explained by the precipitation of CrN that lowers the chromium content in austenite favouring the formation of ferrite/martensite with CrN in a lamellar structure [4, 9, 18]. When the nitriding temperature is increased above 500 ºC Figure (7d), the dark nitrided layers produced have complex structures with various phases including γ – Fe$_{2-3}$N nitride, γ ', CrN, Cr$_2$ γ, γ and interstitial N in γ as shown in Table (3).

From the morphological (Figure (6) and Table (2)) and XRD (Figure (7) and Table (3)) results it can be concluded that gas nitriding of AISI 316L austenitic stainless steel at low temperatures (less than 450 °C) produces bright nitrided layers which are precipitation free and consequently resist corrosion attack. These layers consist of a single phase named S-phase (or expanded austenite, γ $_N$), which is reported to have excellent corrosion resistance [4, 6, 10, 18]. When a critical temperature is reached, CrN (dark phase) starts to precipitate in the original S-phase forming a mixed layer. At higher nitriding temperatures, a dark layer is formed which is mainly composed of fine CrN precipitates in the austenite matrix. Some nitrided microstructures appear as three distinct structural zones as shown in Figure (8). The outside zone is a thin white layer known as the compound zone, which consists of γ' and γ nitrides. The second zone contains austenite, ferrite/martensite and CrN/Cr$_2$N, and is called the diffusion zone, while the third zone is very thin and consists of an interstitial solution of nitrogen in austenite matrix.
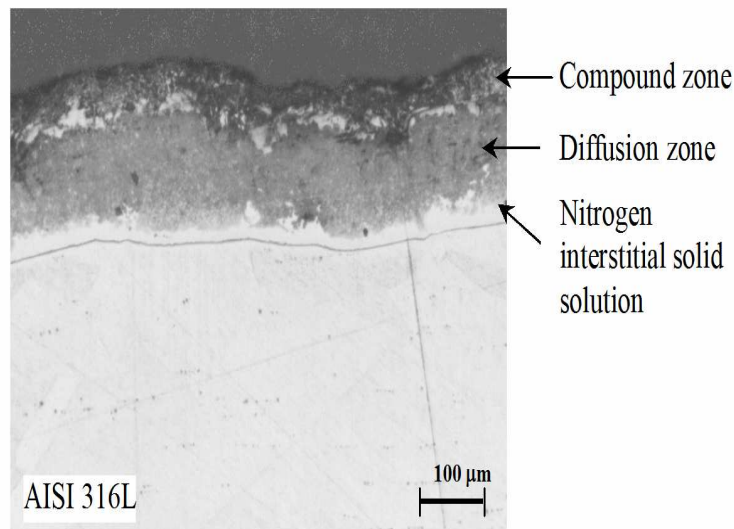

Figure 8: Optical micrograph of a nitrided layer of different structural zones

Surface Hardness Results

The results of the surface hardness measurements of gas nitrided AISI 316L austenitic stainless steel in terms of $HV_{0.1}$ are shown in Table (3). It can be seen from this table that nitriding can increase the surface hardness of the untreated material by more than five times which is of great importance in improving the wear resistance (see Table (3), design points #8 and #15). It is being observed that all specimens (design points) are acceptable from the IGC performance point of view. However a compromise can be made if S-phase is required to be present for some applications but with a surface hardness value in the range of about 600 to 1000 $HV_{0.1}$, (see Table (3), and design points #1, #5 and #11).

Surface Hardness Optimization

Using response surface methodology (RSM) provides the possibility to optimize the surface hardness results of the gas nitrided AISI 316L stainless steel using the response optimizer of MINITAB software. Figure (9) shows the optimization chart for the surface hardness results. This chart predicts that the optimum process parameters setting is 30.2 hr for nitriding time, 533.5 °C for nitriding temperature and 600 L/hr for ammonia flow rate, which would result in an optimum predictable surface hardness of 1294 $HV_{0.1}$. This result represents an increase by a factor of 6.47 as compared with the untreated material surface hardness. The optimization result is based on a regression model and the actual measured values could be somewhat different. Therefore, it is suggested that the optimum settings be implemented in the future and repeated few times to confirm or otherwise refine the obtained result.

Table 3: Surface hardness measurements of the nitrided 316L

Design point	Time	Temperature	Flow rate	Surface hardness $VH_{0.1}$	Phases composition of the nitride layer
1	18	440	200	755	S-phase
2	42	440	200	1026	S-phase, CrN,(
3	18	560	200	1163	CrN,(
4	42	560	200	1139	CrN,(
5	18	440	500	972	S-phase
6	42	440	500	1144	S-phase, (', CrN,(
7	18	560	500	1200	(', CrN,(
8	42	560	500	1243	(', CrN,(
9	10	500	350	1159	S-phase, (', CrN,(
10	50	500	350	1128	(', CrN,(
11	30	400	350	692	S-phase
12	30	600	350	1129	CrN,(
13	30	500	100	1198	(',CrN,(
14	30	500	600	1202	(', (, Cr$_2$N, CrN,(,
15	30	500	350	1240	(', CrN,(
6	30	500	350	1191	(', CrN,(
17	30	500	350	1174	(', CrN,(
Untreated	-	-	-	200	-

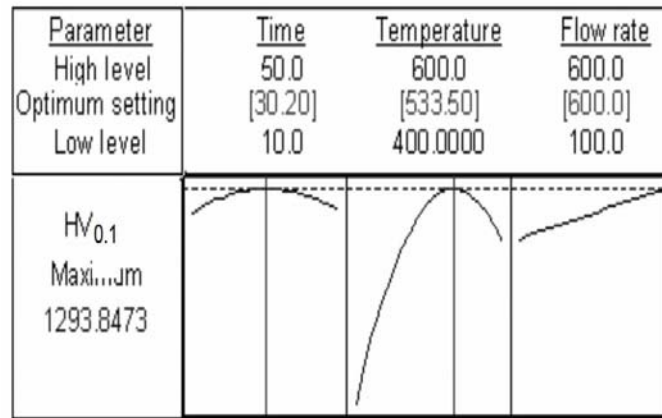| Parameter	Time	Temperature	Flow rate
High level	50.0	600.0	600.0
Optimum setting	[30.20]	[533.50]	[600.0]
Low level	10.0	400.0000	100.0

$HV_{0.1}$
Maxi...um
1293.8473

Figure 9: Response optimization chart for the maximum surface hardness

CONCLUSIONS

From this experimental study, the following points are concluded:

- The nitrided layers formed in the AISI 304, AISI 316 and AISI 316L austenitic stainless steels are similar in morphology and structure with comparable thickness values.

- For AISI 316L austenitic stainless steel, it is found that gas nitriding for less than 30 hours at nitriding temperatures less than 450 °C produces nitrided layers, free of precipitates and mainly composed of a single phase (S-phase) which has a distorted face-centered crystal structure (mostly fct).

- The development of the S-phase by nitriding process is a significant contribution as this phase is reported to retain the corrosion resistance of the nitrided austenitic stainless steel.

- Type AISI 316L austenitic stainless steel is superior to AISI 304 and 316 types in its resistance to sensitization effect (IGC resistant) during gas nitriding at temperatures higher than about 450 °C, that makes it more suitable to be surface hardened using gas nitriding.

- Gas nitriding of AISI 316L austenitic stainless steel significantly increases the surface hardness level which could be ranked to more than six times as compared with the untreated material. This surface hardness enhancement is believed to increase the wear performance of AISI 316L stainless steel.

REFERENCES

[1] Unterweiser P., Howard E. and James J., Heat Treater's Guide, Standard Practices and Procedures for Steel, (American Society for Metals, Metals Park, Ohio), 1982.

[2] ASM Handbook Committee, ASM Metals Handbook, vol. 4, "Heat Treating", (ASM International Materials Park, Ohio), 1991.

[3] Bell T., Surface Engineering of Austenitic Stainless Steel, Surface Engineering, vol. 18, no. 6, p. 415-422, 2002.

[4] Poirier L., Corre Y. and Lebrun J., Solutions to Improve Surface Hardness of Stainless Steeles Without Loss of Corrosion Resistance, Surface Engineering, vol. 18, no. 6, p. 439-442, 2002.

[5] Ichii K., Fujimura K. and Takase T., Structure of Ion-Nitrided Layer of 18-8 Stainless Steel, Technology Report of Kansai University, vol. 27, p. 135-144, 1986.

[6] Menthe E. and Rie K.T., Further Investigations of the Structure and Properties of Austenitic Stainless Steel after Plasma Nitriding, Surface and Coatings Technology, vol. 116-119, p. 199-204, 1999.

[7] De-Oliveira A., Riofano R., Casteletti L., Tremiliosi G. and Bento C., Effect of the Temperature of Plasma Nitriding in AISI 316L Austenitic Stainless Steel, Revista Brasileira de Aplicações de Vácuo, vol. 22, no. 2, p. 63-66, 2003.

[8] Mingolo N., Tschptschin A. and Pinedo C., On the Formation of Expanded Austenite During Plasma Nitriding of an AISI 316L Austenitic Stainless Steel, Surface and Coatings Technology, vol. 201, p. 4215-4218, 2006.

[9] Yasumaru N., Nature of Y_N Phase Formed with Low Temperature Plasma Nitriding of Austenitic Stainless Steel, Proceeding of Stainless Steel 2000 Conference, Osaka, Japan, (Maney Pub.), p. 229-245, 2001.

[10] Bell, T. and Li, C.X., Stainless Steel Low Temperature Nitriding and Carburizing, Advanced Materials and Processes, vol. 160, no. 6, p. 49-51, 2002.

[11] Honeycombe R.W.K., Steels; Microstructure and Properties (Edward Arnold, London), 1981.

[12] ASM Handbook Committee, ASM Metals Handbook, vol. 13, "Corrosion", (ASM International Materials Park, Ohio), 1992.

[13] ASTM Committee, "A262-86 Standard Practices for Detecting Susceptibility to Intergranular Attack in Austenitic Stainless Steels", Annual Book of ASTM Standards, vol. 03.02, p. 1-18. (ASTM, Philadelphia), 1988.

[14] ASTM Committee, "E3-80 Standard Methods of Preparing of Metallographic Specimens", Annual Book of ASTM Standards, vol. 03.01, p. 74-78. (ASTM, Philadelphia), 1988.

[15] ASM Handbook Committee, ASM Metals Handbook, vol. 13A, " Corrosion: Fundamentals, Testing, and Protection", (ASM International Materials Park,

[16] Xiaolei X., Liang W. Zhiwei Y. and Zukun H., A comparative study on microstructure of the plasma-nitrided layers on austenitic stainless steel and pure Fe, Surface and Coatings Technology, vol. 192, p. 220-224, 2005.

[17] Lei M.K. , Phase Transformations in Plasma Source Ion Nitrided Austenitic Stainless Steel at Low Temperature, Journal of Materials Science, vol.34, no.24, p. 5975-5982, 1999.

[18] Zhang Z.L. and Bell T., Structure and Corrosion Resistance of Plasma Nitrided Stainless Steel, Surface Engineering, vol. 1, no. 2, p. 131-136, 1985.